ELSEVIER

Journal of Alloys and Compounds 275–277 (1998) 721–724

Journal of ALLOYS AND COMPOUNDS

Fluorite structural principles: disordered α-phase to ordered intermediate phases in praseodymia

Z.C. Kang, L. Eyring*

Department of Chemistry and Biochemistry, Arizona State University, Tempe, AZ 85287-1604, USA

Abstract

Experimental observations of the structural changes effected during rapid cooling of α-phase praseodymium oxide of various compositions in their ambient oxygen pressure have been reported. These results are discussed in terms of the recently discovered structural principles for the anion-deficient, fluorite-related rare earth higher oxides. Two new polymorphs of the β-phase of praseodymia were found in the experiments, and their structures are now predicted using the new structural principles. Furthermore, the structure of one of two new π-phase polymorphs, Pr_nO_{2n-2m}, that were discovered, π(1) $R_{16}O_{30}$ (n=16, m=1), $RO_{1.88}$, is predicted. The transformation of the established β(1)-phase in the praseodymium oxides to the newly observed β(3)-phase, found in the quenching experiments, is modeled. Finally the surfaces of β(1)- and the α-phase are compared. It is observed that the superstructure of β(1) is clearly reflected in its surface structure. © 1998 Elsevier Science S.A.

Keywords: Modeling of fluorite-type phase transformations; Higher rare earth oxides; Oxygen-deficient fluorite-type oxides; Surface reconstruction in fluorite-type oxides

1. Introduction

The praseodymium α-phase is one of the most extensive nonstoichiometric phases known. The width of the phase is $PrO_{1.72}$ to $PrO_{2.00}$, at temperatures ranging from 420 to above 1000°C, when oxygen pressures are between 50 and 750 Torr [1]. Over most of this region the X-ray diffraction patterns show specimens to be the simple fluorite structure. The PrO_x–O_2 phase diagram is shown in Fig. 1.

Over the same composition range at lower temperatures and pressures there exist several members of a homologous series whose generic formula is Pr_nO_{2n-2m}. Small breaks in the free energy plot of the α-phase region suggests some premonitory behavior as the temperatures approach that at which the ordering process occurs [2,3]. Samples of PrO_x, x=1.78–1.833, have been cooled rapidly by dropping quartz tubes containing an α-phase at selected temperatures and oxygen pressures into iced water. The cooled specimens (Table 1) were analyzed by HREM from both electron diffraction patterns and high-resolution images [4]. The results revealed phases that had not previously been seen, as well as evidence of progressive changes that occurred during cooling.

Recently the structural principles that underlie the oxygen-deficient, fluorite-related homologous series in the higher rare earth binary oxides have been found [5,6]. In this paper we shall examine the considerations set forth above in terms of these principles.

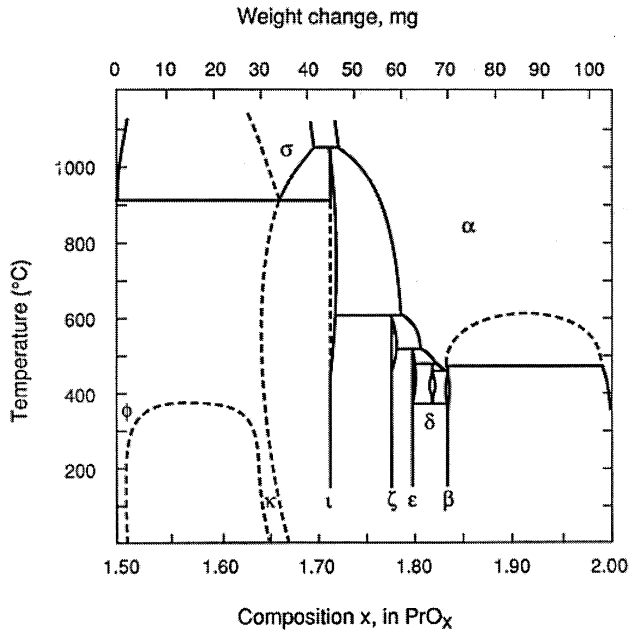

Fig. 1. Phase diagram for PrO_x–O_2.

*Corresponding author. +1 602 9652747; e-mail: leyring@asu.edu

0925-8388/98/$19.00
PII: S0925-8388(98)00428-9

Table 1
Diffraction patterns from quenching α-PrO_x

Run no.	Composition (ratio O/Pr)	Structure observed in several crystals studied; the number indicated is n in Pr_nO_{2n-2m}
1	1.778	9
2	1.78	40, 48(3), 24
3	1.78	α, 40, 12(0), 24(1), 48(3), 16(2)
4	1.79	α, 40, 48(3)
5	1.80	α, 7, 40, 88, 24(1), 48(3), 16(1), 16(3)
6	1.81	α, 40, 12(0)
7	1.82	24(1)
8	1.82	24(1), 48(3)
9	1.83	α, 9, 88, 24(1), 24(2)

There are four known polymorphs of composition O/Pr=1.833: 12(0), 24(1), 24(2), and 48(3). For O/Pr=1.875 there are also polymorphs indicated 16(1), 16(2), and 16(3).

2. The new praseodymia phases

Two new polymorphs of the β-phase were identified. The β-phase of the higher oxides of the rare earths has the composition $PrO_{1.833}$. This is the commonly found end product of the decomposition of some oxygenated salt, such as the oxalate which is heated to 1050°C in air for some hours and allowed to cool slowly to 200°C before placing it in a desiccator. Previously two polymorphs of this phase had been known, β(0), $Pr_{12}O_{22}$, and β(1), $Pr_{24}O_{44}$. In the quenching experiments two more polymorphs were found, β(2), $Pr_{24}O_{44}$, and β(3), $Pr_{48}O_{88}$. Although these last two had not been seen in the praseodymia system they are the most stable phases of this composition that occur in the terbia system. Fig. 2 shows the structures of these four phases. The structure of only that of β(1) has been refined [7]. The structures of the other three have been predicted by the application of the structural principles. (Dr. Kang has introduced these principles and given examples of their application at this conference.) No other polymorphs of the β-phase have been observed.

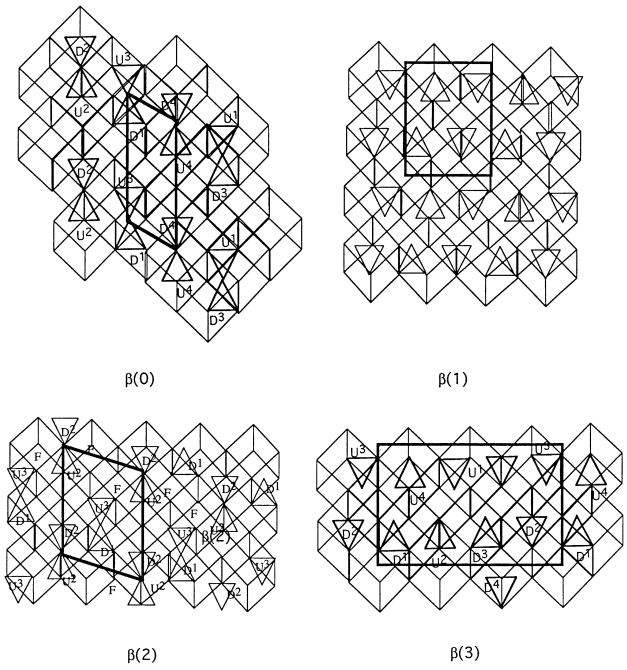

Fig. 2. The structures of the β-phase polymorphs: (a) β(0), $R_{12}O_{22}$, $n=12$ and $m=1$, $RO_{1.833}$; (b) β(1), $R_{24}O_{44}$, $n=24$, and $m=2$, $RO_{1.833}$; (c) β(2), $R_{24}O_{44}$, $n=24$, and $m=2$, $RO_{1.833}$; (d) β(3), $R_{48}O_{88}$, $n=48$ and $m=4$, $RO_{1.833}$.

β(0): $R_{12}O_{22}$, $n=12$ and $m=1$, $RO_{1.833}$

A diffraction pattern of β(0) has 12 intervals along the [351] F direction indicating a unit cell just half that of the β(1)- or β(2)-phases. The modeled ideal structure is given in Fig. 2. The vacancies in this structure are paired (in the first slab there is a pair and two separated vacancies, but when the second, which is similar to the first, is superimposed the other pair is formed), in contrast to their separation in β(1) (Fig. 2).

β(1): $R_{24}O_{44}$, $n=24$, and $m=2$, $RO_{1.833}$

The structure of this phase has been refined from neutron diffraction data [7].

β(2): $R_{24}O_{44}$, $n=24$, and $m=2$, $RO_{1.833}$

The modeled ideal structure is given in Fig. 2 The vacancies occur in pairs which differ from β(1) (Fig. 2), but are similar to those in β(0).

β(3): $R_{48}O_{88}$, $n=48$ and $m=4$, $RO_{1.833}$

In the diffraction pattern the number of the superstructure intervals is doubled in the [220] direction for β(3), but are the same along [111]. The unit cell will then have a doubled *b*-axis but the same *c*-axis. The proposed structure is shown in Fig. 2 with the unit cell highlighted. The modular sequences are very similar between β(1) and β(3), except for an exchange between the second and the fourth modules in the sequence. The unit cell volume of β(3) is double that of β(1). This makes its composition $R_{48}O_{88}$. The modular stacking sequence determines the structure of the phase. As the number of F modules increases the same assortment of modules may have different stacking sequences.

$\pi(1)$, $R_{16}O_{30}$: $n = 16$, $m = 1$, $RO_{1.88}$

The other new phase in this system observed by electron microscopy was $Pr_{16}O_{30}$. (One polymorph of this phase had been seen by HREM in the terbia system [8], and this phase had been suggested by a break in a tensimetric kinetic run and by the simultaneous appearance of a line in the X-ray diffraction pattern observed during the slow oxidation of PrO_x to PrO_2 [9].) Three polymorphs of $Pr_{16}O_{30}$ were observed in the quenching experiment. Patterns of the $\pi(1)$-phase (Fig. 3, top) were sufficient to model its structure utilizing the structural principles (see Fig. 3, bottom).

The composition of $R_{16}O_{30}$ requires eight F modules since, in this case, $m=1$. The electron diffraction pattern (Fig. 3, top) established that the phase observed is the $\pi(1)$ polymorph in the praseodymium and terbium oxide systems [3], but its structure has not been determined. The unit cell revealed by the electron diffraction patterns corresponds to either of two structural sequences, as shown in Fig. 3, bottom. This phase was observed from quenching a disordered sample from high temperature, so it may be metastable.

Together these models utilize the eight types of single vacancies evenly. An intergrowth of the two structures would have a higher energy than either separately. Boundaries are inevitable between the two arrangements which could explain why it is difficult to prepare this phase. Crystals richer in oxygen than $R_{16}O_{30}$ ($RO_{1.875}$) have never been reported. As the number of the F modules increases the possibilities for acceptable modular stacking sequences is dramatically increased and the energy difference between them may become negligible. Such structures would probably be ordered with less precision and a disordered phase would be likely. This is not inconsistent with the phase diagram which shows the β-phase to be stable down to lower temperatures as the composition approaches the fluorite $RO_{2.00}$.

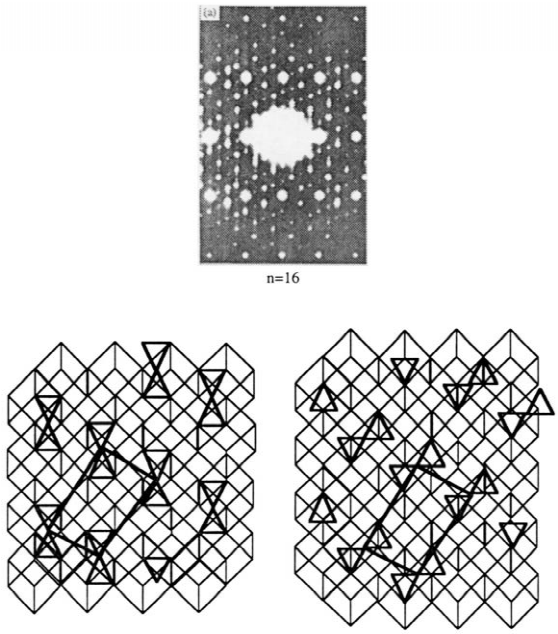

Fig. 3. Diffraction pattern and structure model of of $R_{16}O_{30}$.

3. The phase transformation from β(1) to β(3)

One of the interesting extensions of the structural principle is the capacity to model phase transformations among the ordered intermediate phases. One such transformation is that between β(2) and β(3) given previously in this conference. In Fig. 4 some steps in the transformation of β(1) to β(3) are modeled. Keep in mind that the two phases contain the same set of modules. They differ only in the number of sets of eight vacancies and the stacking sequence which is dictated by the electron diffraction information. This transformation is modeled by considering the possible changes in the successive steps that will conserve the modular set yet bring about the transformation.

4. Surface structures

Because of the importance of the fluorite-related oxides in catalysis it is instructive to examine the surface and near-surface regions of the phases that are considered here. Fig. 5a shows a high-resolution profile image of a precursor to an ordered β(1)-phase just before transformation in the microscope. Fig. 5b is an image of the same surface after ordering to β(1), in situ, in the microscope. Notice in Fig. 5b that the near-surface structure, characteristic of the β(1), is continued clear to the surface. This suggests that surface structure could be modified by the adjustment of the preparative procedures.

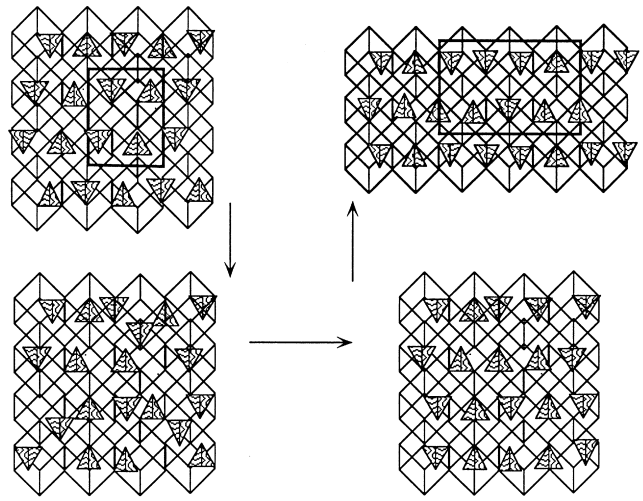

Fig. 4. The modeled transformation of β(1) to β(3).

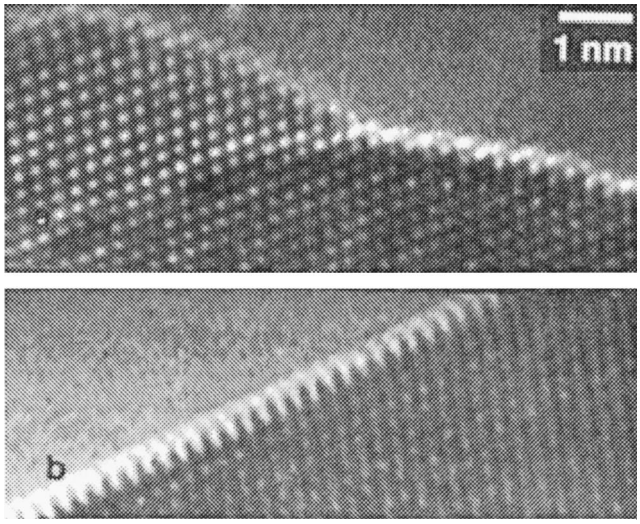

Fig. 5. Surface profile images of (a) PrO_2, (b) $PrO_{1.833}$, β(1), showing the effect of the near surface structure on the surface.

Acknowledgements

We are grateful to Arizona State University for the grant that supported one of us (Z.C. Kang).

References

[1] B.G. Hyde, D.J.M. Bevan, L. Eyring, Phil. Trans. Roy. Soc. (London) A259 (1956) 583.
[2] M.S. Jenkins, R.P. Turcotte, L. Eyring, in: L. Eyring and M. O'Keeffe (Eds.), The Chemistry of Extended Defects in Non-Metallic Solids, North-Holland, Amsterdam, 1970, p. 36.
[3] F.J. Lincoln, J.R. Sellar, B.G. Hyde, J. Solid State Chem. 74 (1988) 268.
[4] Z.C. Kang, J. Zhang, L. Eyring, Aust. J. Chem. 45 (1992) 1499.
[5] Z.C. Kang, L. Eyring, Aust. J. Chem. 49 (1997) 981.
[6] Z.C. Kang, L. Eyring, J. Alloys Compounds 249 (1997) 206.
[7] J. Zhang, R.B. Von Dreele, L. Eyring, J. Solid State Chem. 122 (1996) 53.
[8] R.T. Tuenge, L. Eyring, J. Solid State Chem. 41 (1996) 74.
[9] K. Otsuka, M. Kunitomi, T. Saito, Inorg. Chim. Acta 115 (1986) L31.